

ENVISAT Microwave Radiometer Assessment Report

Cycle 026

13-04-2004 – 17-05-2004

| | | |
|---------------|---|--|
| Prepared by : | M. DEDIEU, CETP L. EYMARD, CETP/LODYC E. OBLIGIS, CLS N. TRAN, CLS | |
| Checked by : | L. EYMARD, CETP/LODYC | |
| Approved by : | P. FEMENIAS, ESA | |



Contents

| | | |
|----------|--|-----------|
| 1 | Introduction | 2 |
| 2 | Maps of the brightness temperatures over South Pole | 3 |
| 3 | Monitoring of the radiometer internal parameters | 5 |
| 4 | Monitoring of cold ocean brightness temperatures | 10 |
| 5 | Conclusion on the cycle assessment and long term monitoring | 11 |
| 6 | Reference documents | 12 |

1 Introduction

This document aims at reporting the behavior of ENVISAT Microwave Radiometer in terms of instrumental characteristics and quality of the brightness temperatures. It is performed on the MWR level 0 data product (MWR_NL_OP). The decoding and the pre-processing are done with the MWR level 1B reference processing chain located at CETP. The data are from the ESA's ground stations in Kiruna, Sweden, and at ESRIN, Italy.

The objectives of this document are :

- to provide an instrumental status
- to check the stability of the instrument
- to report any change at the instrumental level likely to impact quality of the brightness temperatures

It is divided into the following topics:

- **Maps of the brightness temperatures over South Pole**
- **Monitoring of the radiometer internal parameters**
- **Monitoring of cold ocean brightness temperatures**
- **Conclusion on the cycle assessment and long term monitoring**

2 Maps of the brightness temperatures over South Pole

Over poles, the space and time coverages are sufficient to draw maps of the brightness temperatures. Since the atmospheric variability is weak due to the very low water vapour content, the brightness temperatures are mainly representative of surface emissivity and temperature variations, which slowly vary within the course of the year. Consequently, the south pole can be used as a stable target to monitor the brightness temperature variations with time. Figures 1 (top) and (bottom) show respectively the 23.8 and 36.5 GHz brightness temperatures measured by the radiometer over the South pole (latitudes higher than 65°S) for the current cycle. The ice cap appears colder than the sea ice and the free water at the two frequencies.

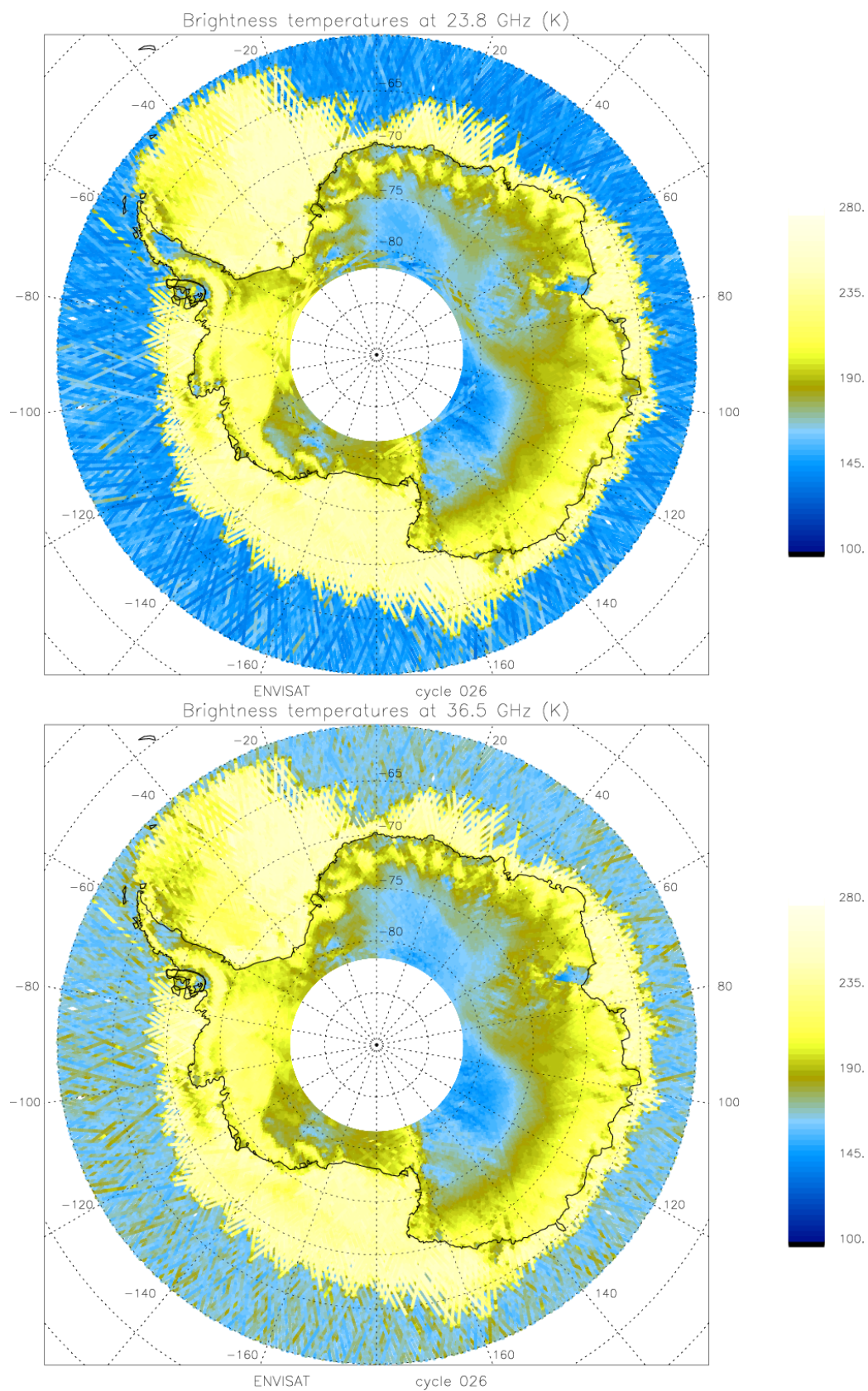


Figure 1: Brightness temperature maps over the South Pole for the two frequencies, 23.8 and 36.5 GHz.

3 Monitoring of the radiometer internal parameters

The radiometer telemetry primarily contains the radiometer counts for each channel, which are related to the brightness temperatures of the main antenna and the two calibration loads, through the working model (Bernard et al, 1993) summarized below:

$$\mathbf{Tfc} = acc \ ah0 \ \mathbf{TC} + (1 - acc) \ ah0 \ \mathbf{Tcc} + (1 - ah0) \ \mathbf{Th}$$

$$\mathbf{G} = (Cc - Cf) / [ao + af \ \mathbf{Tfc} - ac \ \mathbf{Tc} + ah \ \mathbf{Th}/c]$$

$$\mathbf{TE} = (Cc - off) / \mathbf{G} - aref \ \mathbf{Tref} - ad \ \mathbf{Td} + a2 \ \mathbf{Tfc} + a3 \ \mathbf{Th}/c + a4 \ \mathbf{Tc} + a6 \ \mathbf{Tcal} + a5$$

$$\mathbf{T'a} = b1 \ \mathbf{Tref} + b2 \ \mathbf{Td} - b3 \ \mathbf{Tcal} - b4 \ \mathbf{Tc} + \mathbf{TE} - (Ca - off) / \mathbf{G}$$

$$\mathbf{Ta} = c1 \ \mathbf{T'a} - c2 \ \mathbf{Tr}$$

where the coefficients are derived from the primary coefficients shown in figure 2. The brightness temperature is then derived from the antenna measurement, by accounting for the reflector losses and side lobe contributions.

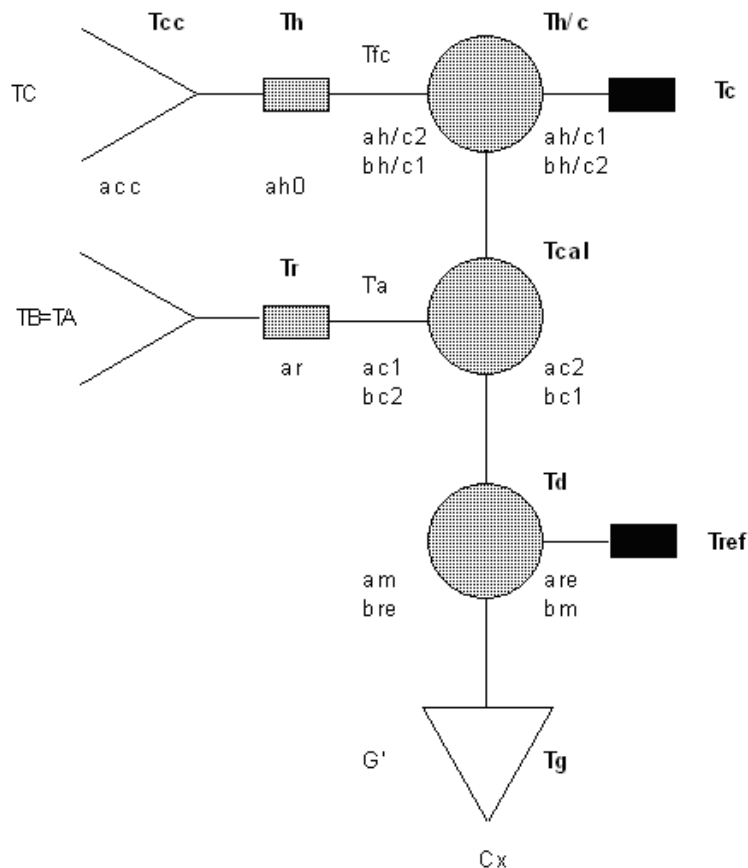


Figure 2: scheme of one channel of the MWR, showing the main antenna, whose measurement is TA, the two calibration loads, consisting of an internal hot load and a sky horn, the reference load (Dicke load - temperature Tref) and internal switches to get every measurement. Each component is characterized by transmission and loss factors which are taken into account in the radiometer model, as well as their temperature.

To monitor the instrument behaviour during its lifetime, the key parameters are plotted in figures 3-5 : gain (after correction of the thermal variations, modeled as a parabolic function),

hot load and sky horn counts, and residual term TE (residual temperature contribution due to errors in the estimated coefficients). The instrument stability is ensured if none of these parameters do vary with time.

The figure 3 (top) shows the gains of the two channels 23.8 and 36.5 GHz, and figure 3 (bottom) is a zoom on the last 10% of time. They show that the gain in the 23.8 GHz channel remains stable around 9.6. For the second channel, the evolution shows two decreasing trends, small at the beginning (starting around day 25) and a stronger one since days around 150 after launch. The total decrease is about 10.6% (at 10.4 at the beginning and 9.30 now). The sky horn counts on figure 4 exhibit similar features than the gain for both channels. The counts present a very slight increase with time for the first channel. For the second channel, the values drop from 3600 to 3250 (-9.7%). The hot load counts on the same figure are stable for the first channel, around 553. They decrease for the second channel from 660 at launch time to about 640 (-3%).

Finally, the last parameter that is monitored, the residual temperature is presented in figure 5. Since launch the values are higher than evaluated from ground testing. The residual temperature was expected to be around 0.5 K for the first channel and a bit higher, 0.5-0.7 K for the second one, i.e. close to the ERS ones (Eymard et al, 2002). There are 4 particular features of this parameter to analyse:

- a drift of the residual temperature at 36.5 GHz, the values are down to -2.5 K with a regular linear decrease since 2-3 months after launch to days around ~450.
- a step is then observed with an increase of 0.5 K. The values were around -2.0 K and are decreasing again and are around -3.0 K.
- a step is observed at 23.8 GHz around day 260 with an increase of 0.5 K.
- a decrease is observed after the previous mentioned step for the 23.8 GHz channel. Since day 450 the values vary around 1.

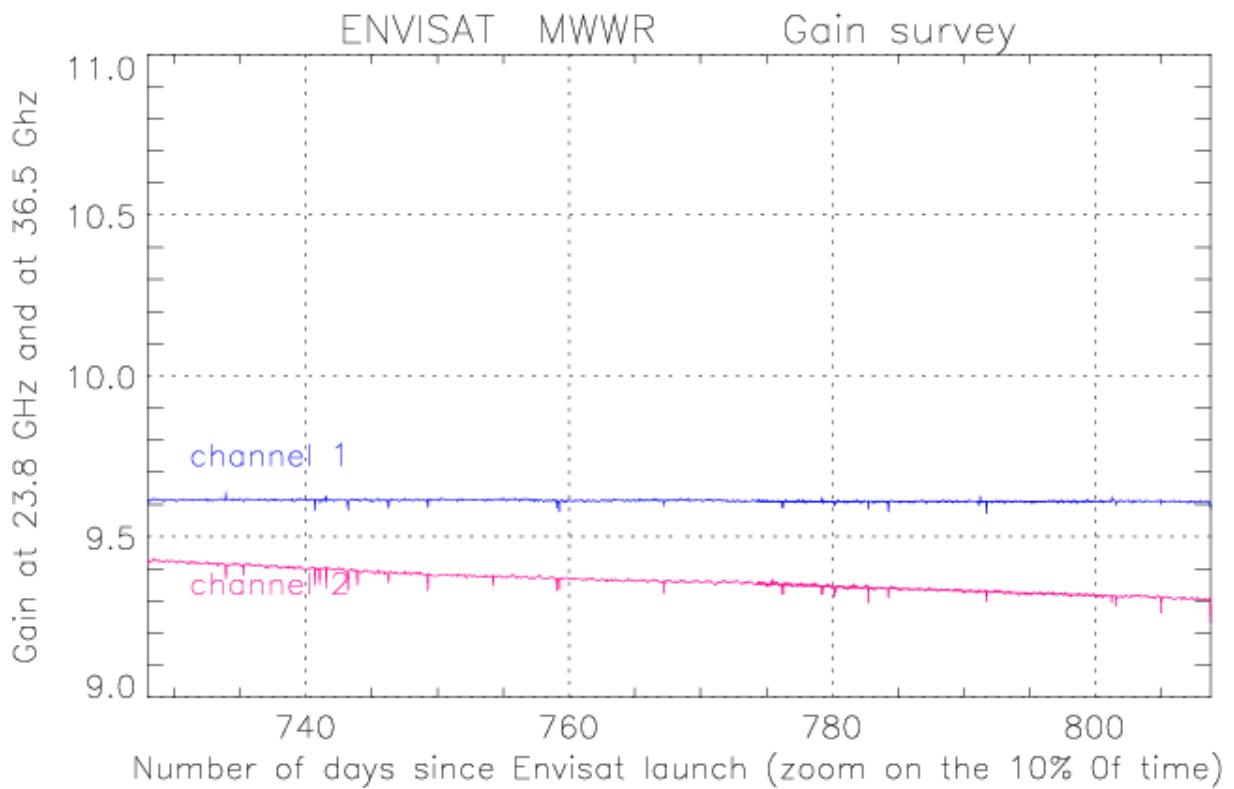
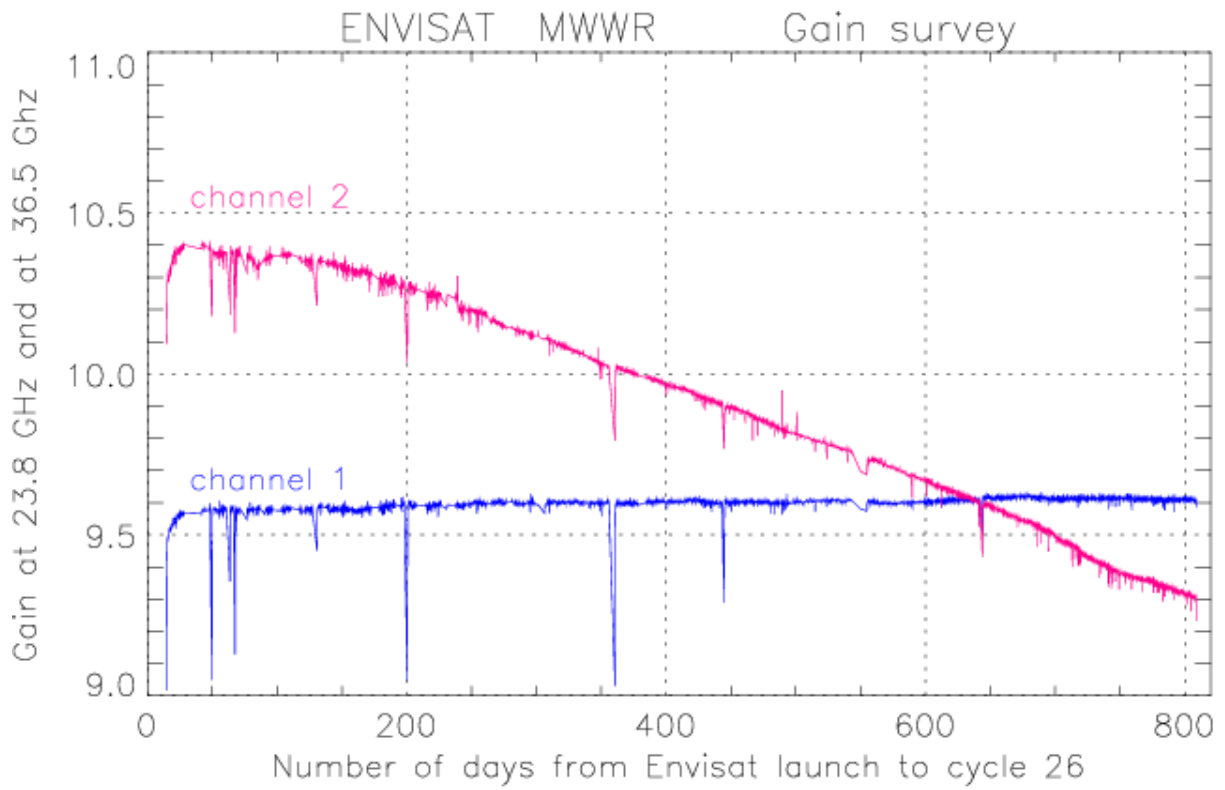


Figure 3: Time evolution of the gain since Envisat launch (March 1st, 2002 - data available since March 15th).

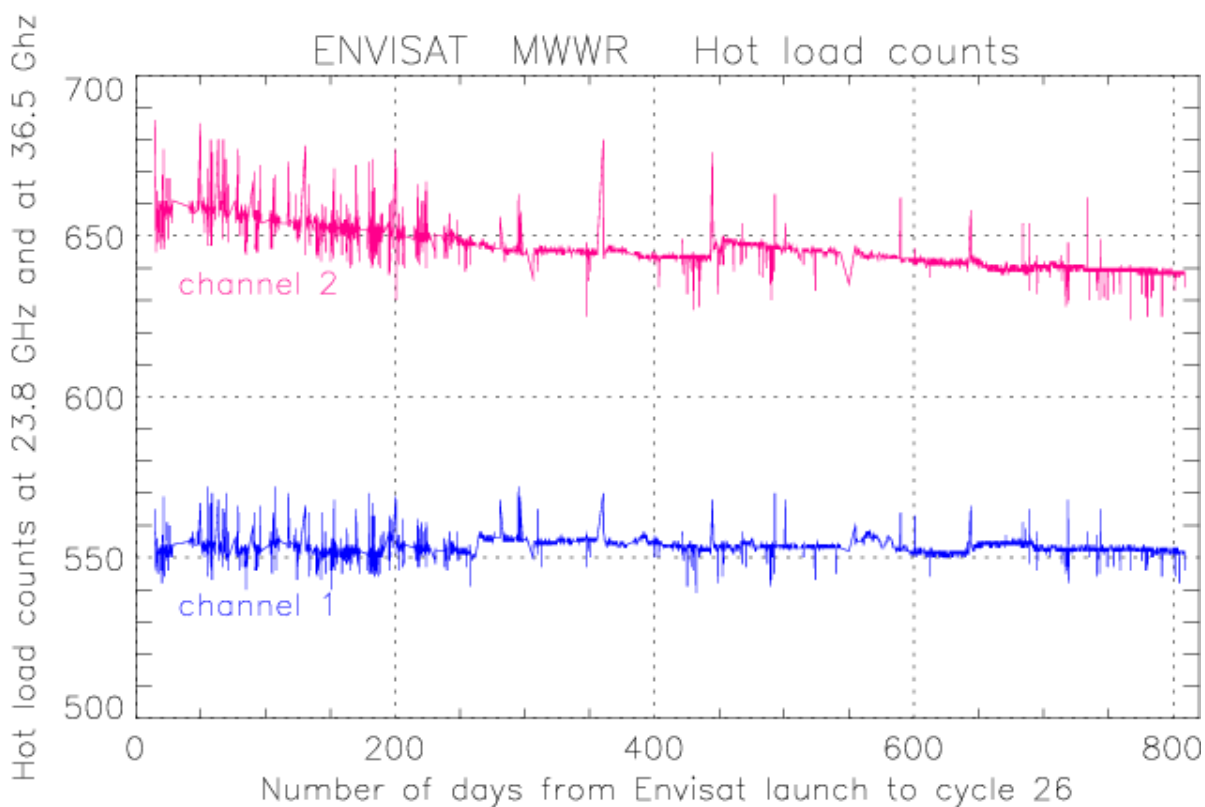
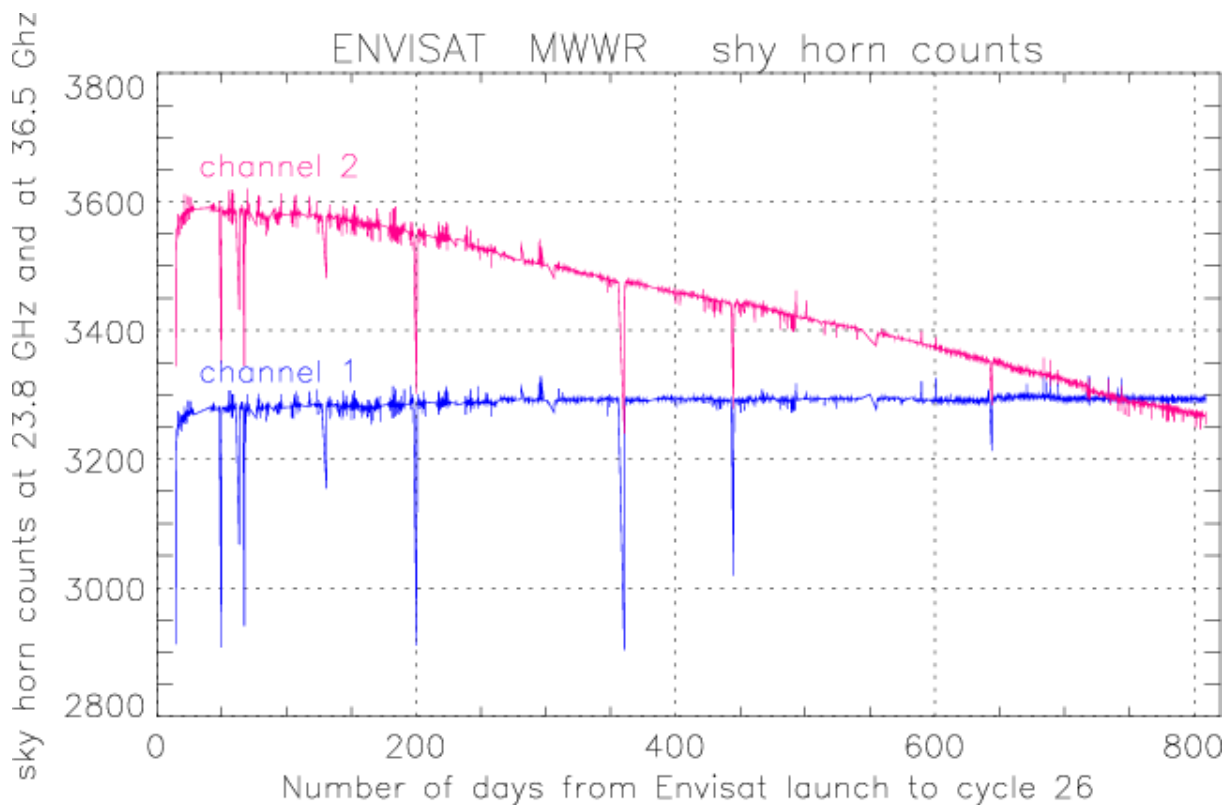


Figure 4: Time evolution of the sky horn count and the hot load count since Envisat launch.

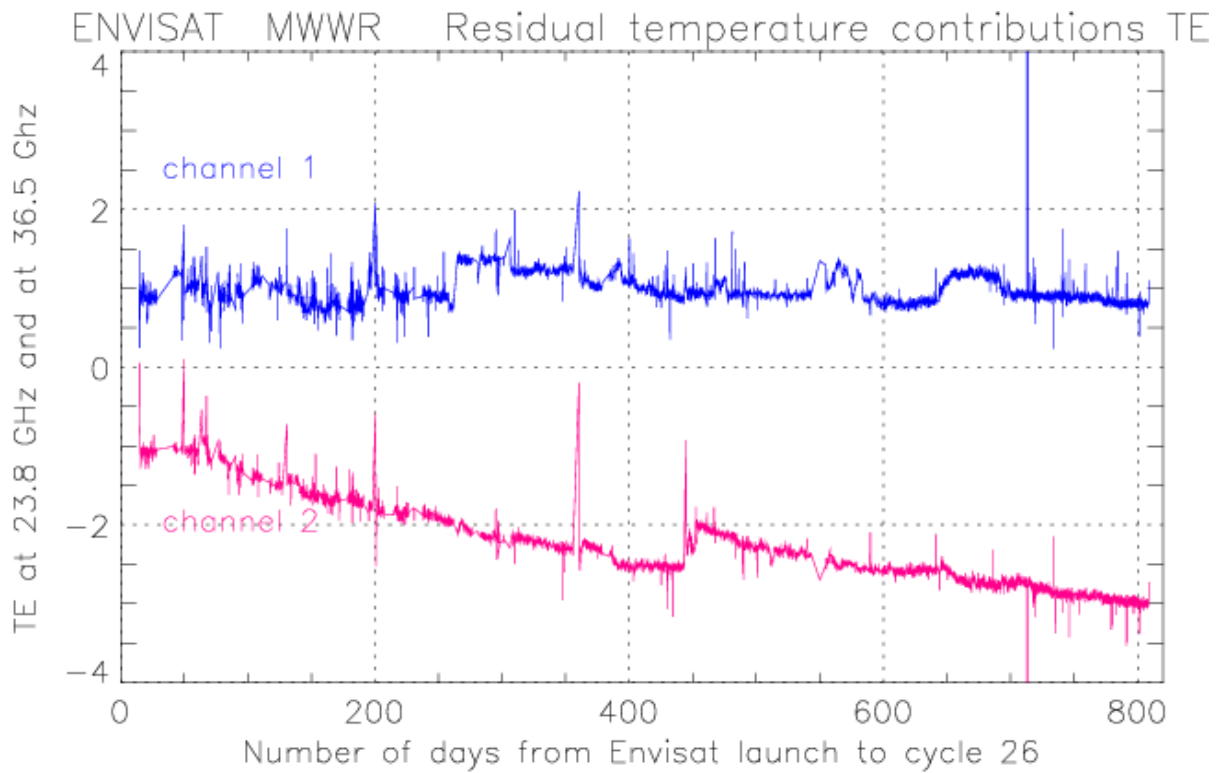


Figure 5: Time evolution of the residual temperature TE, since Envisat launch.

4 Monitoring of cold ocean brightness temperatures

To assess the long term stability of the ERS2 radiometer, monitoring of the two brightness temperatures was performed on several continental areas (Antarctic Plateau, South Greenland plateau, Amazon forest and Sahara desert) and by selecting the coldest measurements over ocean. The latter method, derived from Ruf's one for TMR (Ruf, 2000), was found to be the most efficient to point out the slight trend of ERS2 channel A (Eymard et Obligis, 1999; Eymard et al, 2002). the method consists of first filtering out data with value higher than a given threshold, then filtering out again the remaining data with values above the cycle average minus 1.5 times the standard deviation. Validation of the method was performed by checking its consistency on TMR data (in comparison with Ruf's results).

Following this method developed for the long-term monitoring of ERS2 and using a threshold equal to the average minus the standard deviation, the Envisat resulting time series is plotted in figure 6. For the first channel, the cold ocean TB values present a 0.004 K/year variation, while a variation of 0.383 K/year is observed for the second channel.

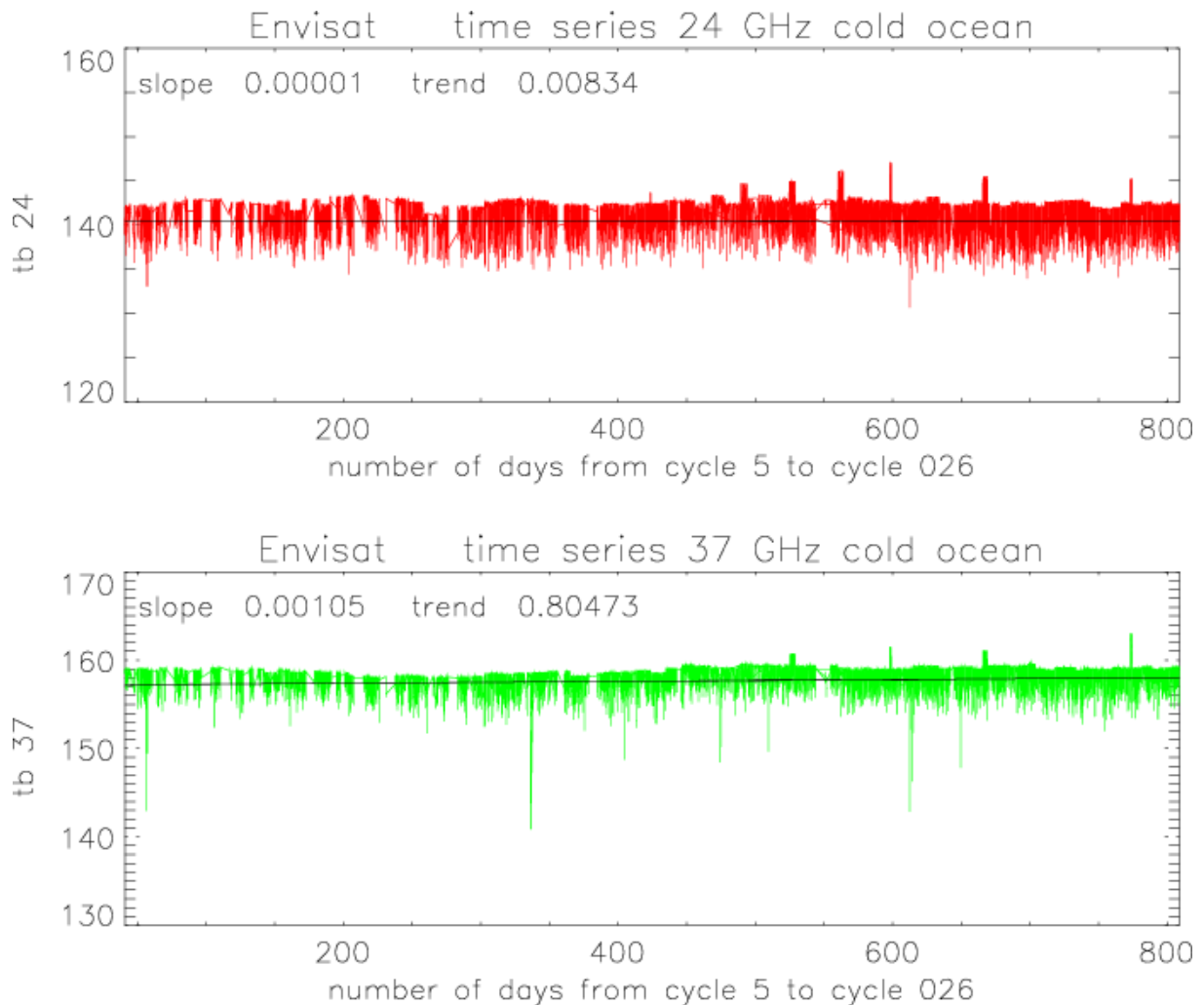


Figure 6: time series of the coldest brightness temperatures over ocean. The x-axis represents the number of days since Envisat launch. The data available before cycle 5 are not used for this monitoring.

5 Conclusion on the cycle assessment and long term monitoring

The monitoring of the main instrumental parameters of the radiometer up to cycle 026 shows a drift of the 36.5 GHz channel. It appears that the gain, the sky horn counts, and the hot load counts have decreased between 3 and 10% since launch. The residual temperature is now 3.0 times higher in absolute value than the one estimated at the beginning of the mission and 4-6 times higher than the one expected from ground testing. No explanation is provided to date.

These features should impact the 36.5 GHz brightness temperature as reported in (Obligis et al, 2003). But as seen in the monitoring of the cold ocean brightness temperatures through the different previous reports the slope of the derived regression line varies at each cycle which makes the quantification of the real impact difficult since the variation observed on the cold TB is a combination of the instrumental features and the annual natural cycle.

6 Reference documents

Bernard et al, The microwave radiometer aboard ERS-1: Part 1 - characteristics and performances, IEEE Trans. Geosci. Remote Sensing, 31(6), 1186-1198, 1993.

Eymard et al, Intercomparison of TMR and ERS/MWR calibrations and drifts, SWT TOPEX-JASON, New Orleans, Oct. 2002.

Eymard et al, Reports on activities performed in 2001 on the ERS2/MWR survey, May 2002.

Eymard et Obligis, Preliminary report on long-term stability of ERS2/MWR over continental areas, 1999.

Obligis et al, Envisat/MWR: 36.5 GHz channel drift status, March 2003.

Ruf, Detection of calibration drifts in spaceborne microwave radiometers using a vicarious cold reference, IEEE Trans. Geosci. Remote Sens., 38(1), 44-52, 2000.